Typical Scenarios of Wave Regimes off Rio Grande do Sul, Southern Brazil

Author(s): Marco A.R. Romeu, José A.S. Fontoura, and Eloi Melo
Source: Journal of Coastal Research, 31(1):61-68.
Published By: Coastal Education and Research Foundation
DOI: http://dx.doi.org/10.2112/JCOASTRES-D-12-00085.1
URL: http://www.bioone.org/doi/full/10.2112/JCOASTRES-D-12-00085.1

Journal of Coastal Research	31	1	61–68	Coconut Creek, Florida	January 2015

Typical Scenarios of Wave Regimes off Rio Grande do Sul, Southern Brazil

Marco A.R. Romeu*, José A.S. Fontoura, and Eloi Melo

Escola de Engenharia, Laboratório de Engenharia Costeira
Universidade Federal do Rio Grande
Rio Grande CEP 96203-900, RS, Brazil

ABSTRACT

Romeu, M.A.R.; Fontoura, J.A.S., and Melo, E., 2015. Typical scenarios of wave regimes off Rio Grande do Sul, southern Brazil. *Journal of Coastal Research,* 31(1), 61–68. Coconut Creek (Florida), ISSN 0749-0208.

In this study, 30 years of sea state data, reconstructed by the wave generation model WWIII for the oceanic area, were used to investigate wave regimes in southern Brazil. By applying a splitting routine to the spectra generated by WaveWatch III (WWIII), each sea state was decomposed into its primary and secondary wave systems. Histograms of the wave height and period against the direction of incidence, constructed for the 30-year period, showed that the region possesses two major wave systems: seas from the E quadrant, and swells from the S quadrant. In a more detailed characterization, histograms constructed with 30 years of data were compared with annual histograms. and the results were used to identify the year that best represented the totality of the data. For the representative year identified, clusters analysis was applied, and six typical scenarios were found for the wave system off Rio Grande do Sul, southern Brazil: (1) E swells, (2) E seas, (3) W seas, (4) S seas, (5) S swells, and (6) SE ground swells. A seasonal analysis revealed that S swells are dominant in the autumn and winter, whereas E quadrant waves (ENE swells and ENE seas) predominate in summer and spring, with more swells in spring and more seas in summer.

ADDITIONAL INDEX WORDS: *Wave regimes, WWIII data, Cluster analysis*.

INTRODUCTION

Ocean surface waves are the main source of energy in open coastal regions. Wave-induced coastal sediment transport, for example, affects coastal features in different time and space scales and is important for coastal engineering and coastal management practices. Ocean waves are a major concern to the safety of human activities at sea, from leisurely sea bathing to professional oceanic operations, such as navigation and offshore oil exploitation. A clear understanding of the wave climate of any given region is, therefore, a subject of great importance to the success of human usage and occupation of the coast.

That general scenario is particularly relevant to the littoral of Rio Grande do Sul, Brazil, for a number of reasons. First, that region is formed by a very long (about 640 km) sandy coastal barrier, with signs of extensive natural erosion in some specific regions (Barletta, 1997; Calliari, Speranski, and Boukareva, 1998). Second, the coast at Rio Grande do Sul is, at the same time, subjected to very small astronomical tides and totally exposed to ocean waves, which makes coastal processes in the area heavily influenced by waves. Third, coastal navigation along that stretch of the Brazilian coast can be quite dangerous because of the lack of harbors, bays, or estuaries to provide shelter in case of necessity. The present study intends to enhance understanding of the wave climate in that area.

Wave climate studies in the past were based on visual ship observations and, whenever available, on instrumental measurements. In recent years, there has been great development in both wave generation and atmospheric models, opening the possibility of using modeled wave data as the basis for wave climate studies, especially in areas where wave measurements are scarce or nonexisting. Among the wave generation models, WaveWatch III (WWIII), used by the National Center for Environmental Prediction (NCEP) of the National Oceanic and Atmospheric Administration (NOAA), became very popular because of the quality of its predictions and its free code for the wind fields necessary to run the model (Tolman, 2002).

As far as the Brazilian coast is concerned, wave climate studies are still in the developing stage. In the following summary, we provide a brief synopsis of some of the previous, related works focusing on the southern Brazilian coast.

Alves and Melo (1999, 2001) analyzed aspects of the wave regime based on 6 months of wave data collected in the shallow waters at São Francisco do Sul island, Santa Catarina (SC) coast, located just North of Rio Grande do Sul (RS) and also part of the southern Brazilian coastal region. Also at Santa Catarina, the first steps in the systematic monitoring of wave climate in Brazil were conducted by the Maritime Hydraulics Laboratory of the Federal University of Santa Catarina. In that monitoring program—the Coastal Information Program (PIC)—systematic wave measurements were collected by a directional Waverider buoy deployed 35 km off the coast of Santa Catarina island at 80 m depth, during 2002 to 2005 (Melo, 2004; Melo *et al.,* 2003).

Along the RS coast, there have been two main wave-monitoring programs so far. In the first, Strauch and Schimidt (1998) measured waves with a directional Waverider buoy deployed in shallow waters (17.5 m depth) for 12 months. The second program was conducted under the guidance of the

DOI: 10.2112/JCOASTRES-D-12-00085.1 received 8 May 2012; accepted in revision 18 January 2013; corrected proofs received 11 April 2013; published pre-print online 1 May 2013.
*Corresponding author: mar7surf@hotmail.com

Brazilian Navy, as part of the National Program for Oceanographic Observation (PNBOIA), and the instrument used was a nondirectional wave gage deployed at 100 m depth. Both campaigns were conducted at sites near the Rio Grande channel in the central part of the RS coast. In the same region, Cuchiara *et al*. (2009) used measurements and modeling to study the effect of a cohesive mud bottom in attenuating wave energy in shallow waters, which turned out to be of great interest for the nearshore wave climate of that part of the RS coast because of the presence of such material brought in from the Patos Lagoon by the Rio Grande channel.

For wave climate studies based only on modeled data, Pianca, Mazzini, and Siegle (2010) used 11 years (1997–2007) of WWIII hindcasts (available from NOAA) for 6 selected (offshore) points along the Brazilian coast to provide a general view of the country's wave climate, which included the southern region.

All previous works contributed to the description of the wave climate in the region of interest. However, for this article, studies carried out by Melo *et al*. (2008), Melo, Romeu, and Hammes (2010), and Araujo *et al*. (2003) deserve special attention. In the first two works, the authors addressed a fundamental point that lies behind the use of modeled wave data for climatic studies, namely, the accuracy of model results for the area at issue. That research was performed by comparing hindcasts of WWIII with NOAA-reanalyzed winds with field measurements obtained during the PIC program at SC (Melo *et al.,* 2008) and during the PNBOIA program at RS (Melo *et al.,* 2010). In both cases, model-by-data comparisons showed that WWIII hindcasts were indeed capable of reproducing measured wave parameters with an accuracy level comparable to that of similar applications done in other parts of the world. These results, therefore, attested to the reliability of WWIII for this part of the south Atlantic Ocean.

The article by Araujo *et al*. (2003) was a source of inspiration for the present work. Among other things, those authors used Cluster Analysis techniques, applied to measured wave data from the PIC program in conjunction with knowledge of meteorological scenarios over the south Atlantic Ocean, to infer valuable information on the characteristic wave regimes of the SC coast. Here, we have used and expanded on the ideas of Araujo *et al*. (2003) to enhance understanding about the waves at the RS coast. To do so, we used the usual statistical properties of wave climate data and sought to use WWIII-derived wave data to identify typical scenarios of wave systems that form the wave climate along the RS coast, which was achieved through a combination of Cluster Analysis and a knowledge of the meteorological patterns associated with the different sea states observed in the region.

METHODOLOGY

Reconstruction of Sea States

The wave generation model, WaveWatch III, used in this study was version 2.2, with all parameters in the default mode. A detailed description of the model is found in Tolman (2002). In brief, WWIII determines the evolution of the directional spectrum of the wave field under the action of a given wind field, taking into account (whenever necessary) the effect of wave refraction. Wind fields used in this work were downloaded from the reanalysis database of NOAA with spatial resolution of 1.00° latitude by 1.25° longitude. WWIII was run in two nested numerical grids: a "global" grid, which encompassed all oceans with 1° by 1.25° resolution, and a "local" grid, with focuses on the southern Atlantic Ocean, at a 0.25° by 0.25° resolution.

The reconstruction of the sea states started on 1 January 1979 and continued until 31 December 2008. The wind field used for calculations was updated every 3 hours. This methodology enabled us to recreate (without any gaps) the offshore sea state conditions for a 30-year period. Modeled wave data were collected on a grid point that coincided with the position of the PNBOIA buoy, located right in the center of the RS coast in waters of 100 m depth (Figure 1). With the 3-hour time step, the data totaled 29,225 output points. At that depth, most waves have not yet been affected by the bottom. In addition, because the dimensions of atmospheric systems that generate waves are typically of the order of a few hundred kilometers and because this reconstructed (offshore) sea state would not show significant variations on a distance scale of a few hundred kilometers, we assumed that conditions at this site were representative of the rest of the RS coast.

Cluster Analysis

The use of synthetic data (*i.e*. obtained from models) to describe the wave climatology of a given site opened possibilities never dreamed of when one had to rely on field measurements only. In fact, as opposed to measurements, synthetic data, nowadays, can easily cover several decades with no interruptions, producing a formidable amount of information. With that information, robust, statistical treatments of wave data became possible, allowing, for example, the construction of wave histograms (wave roses, see next section) for typical wave parameters that describe a sea state: significant wave height (*Hs*), peak period (*Tp*), and peak direction (*Dp*).

Although useful for practical purposes, mere statistical properties of the wave climate may not convey all the valuable information present in the data; therefore, complementary methods of treating the data in a concise way are important. Similar situations in other fields of science led to the use of Cluster Analysis to identify groups of "individuals," within the data set, which shared similar characteristics (see Camus, Mendez, and Medina, 2011 for a recent application). In the following section, we provide a brief description of the Cluster Analysis technique used in this article.

Briefly, *Cluster Analysis* is a partition process for a heterogeneous population, dividing it into a number of homogeneous groups or "clusters." There are no predefined classes in the cluster; elements are grouped according to similar statistical characteristics based on preestablished selection criteria (the reader is referred to specific literature, such as Bijnen [1973] for details on Cluster Analysis theory). The analysis used herein is based on the work of Araujo *et al*. (2003). In this approach, the relevant information for identification of wave scenarios lay in the *Tp* and *Dp* space and, thus, information on *Hs* was not explicitly used, which can be justified because the connection we seek to make with

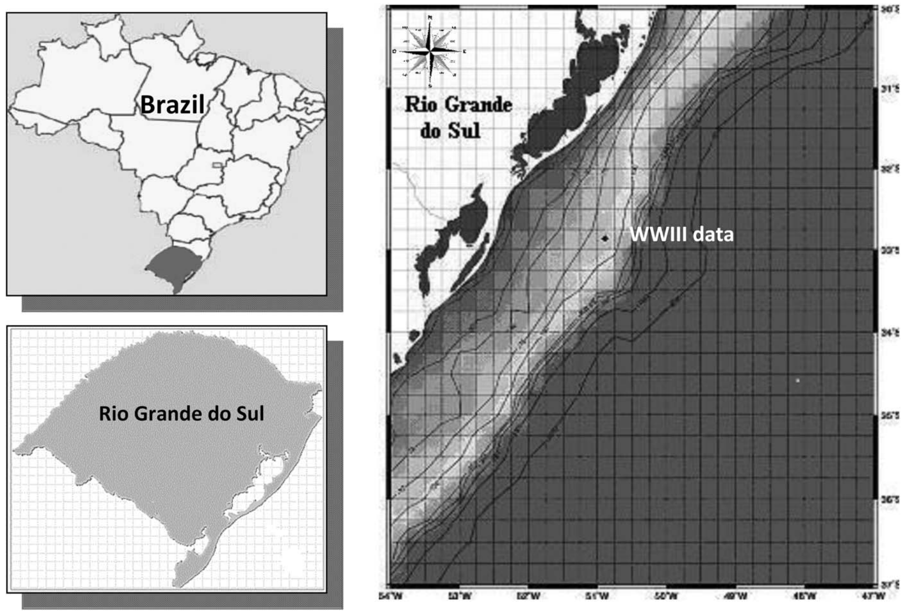

Figure 1. Place where data was collected and calculated by WWIII (32°54′ S, 50°48′ W).

meteorological patterns is better understood with information on period and direction of a given sea state, rather than with its energy content (related to *Hs*).

Araujo *et al*. (2003) used a Mahalanobis metric for distance (*D*) computation:

$$D_{ab}^2 = (x_a - x_b)' S^{-1} (x_a - x_b) \tag{1}$$

Where x_a and x_b are objects and S is the sample covariance matrix. In the case of elementary objects, x_k is a vector in the θ_p, T_p space, whereas for cluster objects, x_k represents the centroid of the cluster k with n_k elements, defined by Equation (2):

$$x_k = \frac{1}{n_k} \sum_{i=1}^{n_k} x_i^k, \qquad x_i^k \in k \tag{2}$$

As a decisional rule for the hierarchical clustering, and still following Araujo *et al*. (2003), we used the Ward's method described in Bijnen (1973), which minimizes the sum of the squared, within-group distance about the group mean of each parameter for all parameters and for all groups simultaneously at each iteration.

Contrary to Araujo *et al*. (2003), the decision for the optimum number of clusters was kept "manual," *i.e*. chosen by the user, and the final number was determined by physical arguments regarding meteorological patterns that are known to occur in the area. This type of approach requires a sound knowledge of the relation between sea states and meteorological scenarios that occur in the area, which arises from extensive analysis of meteorological charts and sea conditions and by practical "seamanship" experience.

RESULTS

As mentioned above, for climatologic studies, the complexity of the wave field in a given sea state is assumed to be well characterized by the parameters *Hs, Tp,* and *Dp,* obtained from the directional spectrum that describes the sea state. This approach tacitly assumes that all sea conditions are composed of single-wave "systems" or, in other words, of single, peaked (unimodal) spectra. As shown shortly, that may not be a good assumption in places frequently subjected to bimodal (or multimodal) sea states.

Nevertheless, our quest for typical scenarios of wave regimes started by constructing histograms for *Hs* and *Tp vs*. direction *Dp* for the entire 30-year data set—which gave rise to the famous "wave roses" if polar coordinates were used. In this first round, we used the *Hs* of a given sea state as the significant wave height, based on the total energy content of the correspondent spectrum (Hs_{TOTAL}), whereas *Tp* and *Dp* were the period and the direction of the most energetic peak in the spectrum (in cases where there were more than one peak present). Results for the Hs_{TOTAL} and *Tp* roses are shown in Figures 2 and 3. (Note that all histograms presented in this study have 24 directional sectors, *i.e*. $\Delta\theta = 15°$, thus, keeping the original directional discretization of the WWIII data).

Both roses showed that there were two main wave systems in the local wave climate: waves from the S quadrant—the most energetic and frequent ones—and waves from the E quadrant. In addition, the *Tp* rose clearly showed that waves from the S quadrant had longer periods (*Tp* above 10 s, typical of swells), whereas waves from the E quadrant tended to have shorter periods (*Tp* below 10 s, typical of seas).

Studies of wind climatology in the area (Tomazelli, 1993) have shown that dominant winds (as a percentage of

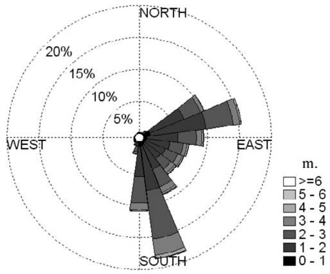

Figure 2. Rose of total significant wave heights (meters) for the entire 30-y data set.

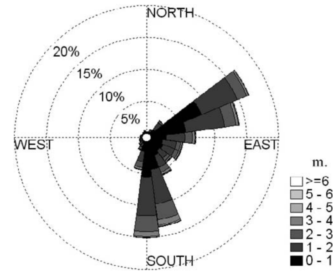

Figure 4. Rose of split significant wave heights (meters) for the entire 30-y data set.

occurrences) are from NE, whereas the most-intense winds come from WSW. Waves from the E quadrant, therefore, find correlation with (local) NE winds, confirming that this wave system, or at least part of it, must have local generation. On the other hand, (persistent) waves from the S quadrant did not have a persistent S wind counterpart, which indicates that most of those waves were swells, generated in higher latitudes. Waves from the WSW direction, whose winds were the most intense, barely appear in the roses because of the obvious fetch limitation caused by the continent.

Because southerly waves did not show much correlation with local winds, one may wonder about the possibility of finding S swells and E seas simultaneously present in the area. This bimodality of sea state conditions in southern Brazil was addressed by Araujo *et al*. (2003), who showed, based on field data from SC, that NE seas and S swells are simultaneously present 30% of the time. Clearly, bimodal structures of the wave climate in the area should not be overlooked.

To better evaluate that issue, we applied a splitting routine in our data set (called *Wsplit*), which is part of the WWIII package. The routine identifies independent wave systems in the directional spectrum and calculates the trio of parameters, *Hs, Tp,* and *Dp,* for each one of them. That procedure enabled data on seas and swells (and even different swells), which eventually occurred simultaneously, to be split and considered as independent wave system, under, of course, a linearity assumption.

In the second stage, we recalculated our directional histograms using that separated wave data set. New roses with *Hs, Tp,* and *Dp,* taken from the new split-wave systems, were constructed and are shown in the Figures 4 and 5.

A comparison between "total" (Figures 2 and 3) and "split" (Figures 4 and 5) wave roses shows that the splitting procedure decreased the percentage of occurrence of SSE wave systems and increased the percentage of occurrence of S and ENE wave systems. Therefore, part of the original SSE conditions may have actually contained the secondary wave systems from the S and/or ENE sectors. As a result, after the splitting, wave roses (Figures 4 and 5) displayed a more-balanced distribution of occurrences between the two dominant sectors, with the percentages of occurrence for both being about 30% each. The splitting also caused an overall decrease in the magnitude of significant wave heights in the *Hs* rose (see Figures 2 and 4) because of a redistribution of wave energy among wave systems.

Wave roses provided important information regarding the ubiquitous presence of swells from the S and seas from the NE on the local wave climate, but still did not convey the detailed scenario structure we looked for. Therefore, to advance further we used the Cluster Analysis technique described in the previous section. All subsequent analysis was done with the "split" wave systems.

The first obstacle we had was the number of data points available for the clustering analysis. Performing the analysis with the whole 30 years of (split) data was impractical because of the enormous computational effort required. In fact, the clustering technique demands the calculation of a similarity measurement among the elements that are supposed to be grouped, which dramatically increases the number of "individuals."

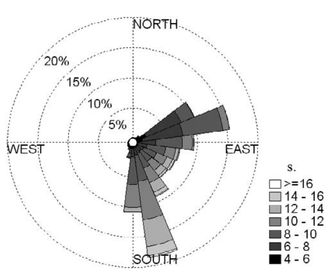

Figure 3. Rose of peak periods (seconds) for the entire 30-y data set.

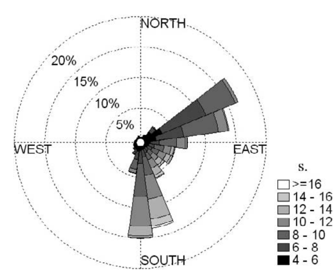

Figure 5. Rose of split periods (seconds) for the entire 30-y data set.

Table 1. *Values of mean standard deviation for annual relative frequencies*.

Year	SD
1979	0.0089
1980	0.0101
1981	0.0105
1982	0.0112
1983	0.0093
1984[a]	**0.0082**
1985	0.009
1986	0.0103
1987	0.009
1988	0.0113
1989	0.0112
1990	0.0091
1991	0.0094
1992	0.0104
1993	0.0106
1994	0.0103
1995	0.0116
1996	0.0111
1997	0.0096
1998	0.0103
1999	0.0098
2000	0.0084
2001	0.01
2002	0.0101
2003	0.0106
2004	0.009
2005	0.0092
2006	0.0092
2007	0.0095
2008	0.0115

[a]Representative year.

The alternative we used was to identify the year that best represented the entire data set and applied the clustering analysis to only that single representative year. Using the directional histograms of the entire 30 years of data as reference, we compared similar histograms made for each year to find the year that had the greatest similarity with that of the total set. To perform the comparison, equivalent matrices of standard deviations of relative frequencies for every annual histogram were calculated. Next, based on those matrices of standard deviation, mean standard deviations were determined for every year, and the year with the lowest mean standard deviation (1984) was chosen as the representative year. Table 1 displays the mean standard deviations found for the annual histograms.

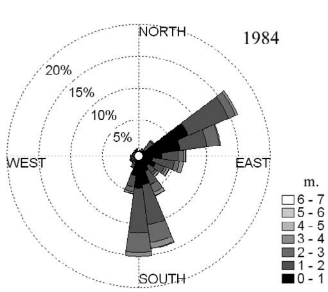

Figure 6. Rose of split significant wave heights (meters) for 1984.

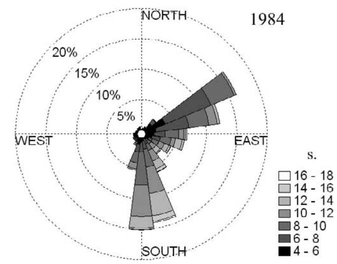

Figure 7. Rose of split periods (seconds) for 1984.

The wave roses for the identified year (1984), chosen as representative of the entire data set, are shown in Figures 6 and 7.

We can attest to the success of the procedure by comparing Figures 4–7. The histograms for the year 1984 present the same balanced distribution of occurrences between dominant sectors, with a percentage of occurrences of about 30% each. The wave height range for 1984 is also similar to the one found for the entire data set.

Identification of Typical Scenarios

Having selected 1984 as the representative year for the period, the clustering technique was applied to a set of about 4000 pairs of *Tp, Dp* points belonging to that year, and the result is shown in Figure 5. As mentioned, the number of clusters—six—was chosen based on the authors' knowledge of local sea conditions. So, the results of the analysis for the six clusters identified are shown in Figure 8.

Thus, by adding information provided by the Cluster Analysis, along with the results presented in Araujo *et al.* (2003) and local knowledge of sea state functioning in the region, we were able to identify six typical wave scenarios for the region, as summarized in Table 2.

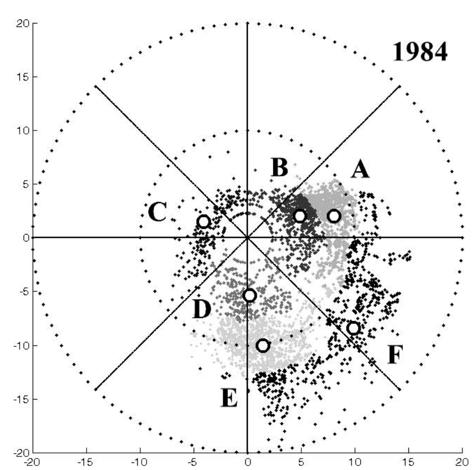

Figure 8. Dispersion diagram of $Tp \times Dp$ for 1984 with six clusters identified. Directions are taken as follows: N = 0° (↑); E = 90° (→); and circles represent the center of gravity (CG) for each cluster (see Table 2 for precise location of CGs).

Table 2. *Wave regime scenarios; types of wave systems; maximum, position of the gravity center, minimum, and standard deviation for direction and period; maximum, mean, minimum, and standard deviation for* Hs*; and the percentage of the occurrence of each cluster*.

Scenario and Parameters	Type	*Dp* (N°)	*Tp* (s)	*Hs* (m)	% Occurrence (annual)
A	ENE swell				25.80
Maximum		141.40	10.79	4.43	
Gravity center		75.53	8.30		
Mean				1.02	
Minimum		32.9	6.49	0.15	
SD		17.03	0.95	0.90	
B	ENE sea				16.91
Maximum		131.12	7.36	3.00	
Gravity center		67.20	5.27		
Mean				0.98	
Minimum		1.84	4.02	0.15	
SD		22.28	0.78	0.52	
C	W sea				5.55
Maximum		359.63	9.09	4.67	
Gravity center		290.37	4.38		
Mean				1.62	
Minimum		219.99	4.00	0.15	
SD		39.07	1.14	0.89	
D	S seas				8.64
Maximum		232.36	7.85	3.41	
Gravity center		178.03	5.37		
Mean				0.94	
Minimum		135.95	4.00	0.16	
SD		20.33	1.10	0.68	
E	S swell				27.26
Maximum		214.48	12.80	4.82	
Gravity center		171.75	10.12		
Mean				1.11	
Minimum		119.82	7.52	0.15	
SD		16.04	1.28	0.85	
F	SE swell				15.80
Maximum		199.76	19.68	3.83	
Gravity center		130.34	12.97		
Mean				1.04	
Minimum		68.02	9.36	0.15	
SD		29.68	1.89	0.94	

For the sea state "type" (*i.e.* sea or swell), the criteria we used was based on the waves' relation to their generation source, according to the usual concept in which *sea* relates to waves locally generated and *swell* to waves remotely generated. The mean directions and mean periods that appear in Table 2 correspond to the position of the center of gravity for each cluster (see Figure 8), whereas the associated mean height was calculated by a simple average of all *Hs* belonging to the corresponding cluster points (*Dp, Tp*). A general idea about the range of variation for each parameter within each scenario is also indicated through the maximum, minimum, and standard deviation of the parameters corresponding to each cluster. Finally, the annual percentage of occurrence of each one of the six scenarios is presented. That percentage includes the simultaneous occurrence of different wave systems.

As an example of the usefulness of these wave-regime scenarios, this methodology is used in the next section to assess seasonal characteristics of the wave climate.

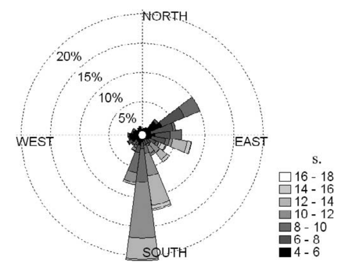

Figure 9. Rose of split periods (seconds) for autumn 1984.

Seasonal Characteristics Interpreted from a Wave-Scenario Perspective

The seasonal characteristics of the wave climate in 1984 can also be evaluated by the wave roses and by the diagram of their cluster dispersion (See Figures 9–12).

DISCUSSION

Here, we briefly discuss the meteorological patterns related to each wave scenario. Scenarios A and B are related to the persistent ENE winds associated with high pressure systems typical in the region. Scenario B are for waves of shorter periods generated near the coast. Scenario A is an evolution of scenario B, which arise when winds from the east quadrant intensify, and the fetch increases.

Scenario C is made up of waves that propagate from the continent toward the ocean and do not exist at the shoreline, and are, therefore, of little interest for coastal studies. They are generated by offshore winds (*i.e.* from the west quadrant), which usually occur just before the entrance of a cold front or of a low-pressure system in the region. This scenario was captured by WWIII because the output point we used was located about 100 km offshore. The value of the parameters associated with this wave system decreases as distance to the coast decreases, reaching zero at the shoreline.

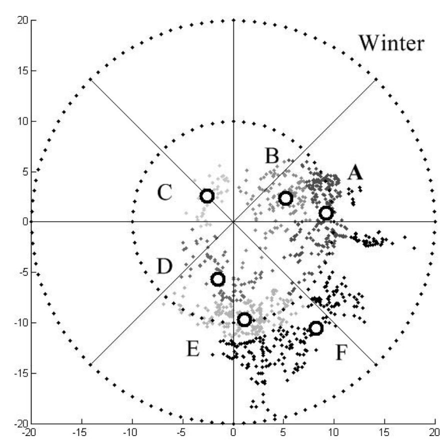

Figure 10. Dispersion diagram of $Tp \times Dp$ for the winter 1984 with six clusters identified.

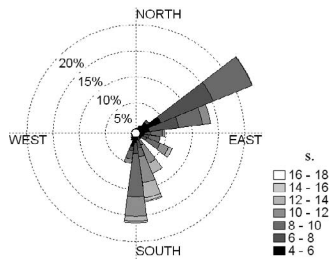

Figure 11. Rose of split periods (seconds) for spring 1984.

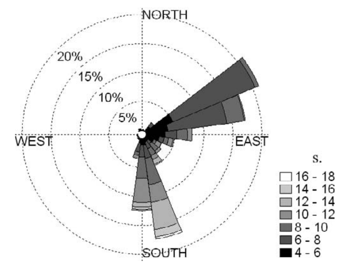

Figure 12. Rose of split periods (seconds) for summer 1984.

Scenario D is composed of shorter-period sea waves generated locally along the RS coast by winds from S to SE, which usually occur during the passage of cold fronts. This scenario can evolve, in some cases, to scenario E (described next), depending on the evolution and intensity of the cold front.

Scenario E consists of swells generated by winds from the south quadrant that happen further south. These winds are caused by cold fronts or, in the more-energetic cases, by extratropical (E-T) cyclones that develop over the ocean off the Uruguayan and/or Argentinean coasts. By looking at the corresponding Hs_{MAX} and Tp_{MAX} (see Table 2), we find that the most severe sea states in the area belong to this scenario. Melo *et al*. (2010) analyzed extreme sea state conditions in the area and concluded that the most intense ones result from E-T cyclones. When it comes to extreme conditions, the importance of E-T cyclones in the RS wave climate must be emphasized. Actually, the relevancy of such meteorological system for the coastal area of the RS goes beyond wind waves. Machado (2011), in a study of storm surges at the RS coast, presented an interesting overview of the paths of E-T cyclones in the region and related them to erosion problems found at the RS coast.

Finally, scenario F refers to longer-period, distant swells, generated by atmospheric systems that eventually form in higher latitudes of the south Atlantic Ocean.

The boundaries of the clusters, which define the limits of each wave scenario, involve some unavoidable "grey" zones. In fact, connections among different wave scenarios (*i.e*. one scenario evolving into another) are part of the natural setting of the wave climate, and in some cases, an attempt to classify a given sea state as scenario X or Y may be somewhat artificial or arbitrary. Nevertheless, we believe that the classification proposed herein may be useful in practical applications.

Seasonal Characteristics

From a seasonal point of view, clusters kept similar structures and their gravity centers were in positions that were close to the ones found in the annual analysis. This fact showed that all six scenarios of marine disturbance occurred in all seasons.

Swells from the south quadrant (scenario E) are dominant in autumn and winter, even though they also occur yearlong. However, their typical wave periods increase in winter, and the cluster interweaves with that of scenario F (distant swells from the SE), which also dominates in winter, along with the south swells.

It is also noticeable that, in the winter of 1984, swells outnumbered seas in all directional sectors. There were high wave periods from the S and the SE and from the E quadrant, as well.

The scenarios of the E quadrant predominate in summer and spring, with a large number of ENE swells (scenario A) in spring and mostly ENE seas (scenario B) in summer.

CONCLUSIONS

In this article, synthetic wave data for 30 years were obtained from hindcasts of WWIII, with the objective of identifying the sea state scenarios that compose the wave climate of the oceanic region off the Rio Grande do Sul, Brazil, coast. Because of the frequent, simultaneous occurrence of different wave systems in the area, a splitting routine was applied to identify and separate different wave systems present in all spectra calculated by WWIII.

A statistical analysis based on directional histograms constructed with split wave systems showed a balance between waves from the two dominant directional sectors: S–SSE and NEE–ENE, with nearly equal percentages of occurrence, close to 30%, and higher occurrence of seas from the east quadrant and swells from south quadrant.

To identify the sea state regimes that compose the local wave climate, we used a combination of a Cluster Analysis technique, applied to pairs of *Tp, Dp* parameters, with local practical knowledge of sea state by meteorological patterns over the area. Because of computational limitations, that technique could not be applied to the full 30-year data set, and we had to devise a method of finding the year that best represented the entire data set. An analysis for that representative year—1984—allowed us to identify six wave-regime scenarios: (1) E swells, (2) E seas, (3) W seas, (4) S seas, (5) S swells, and (6) SE swells.

A seasonal analysis of the wave climate performed with the wave-regime perspective for the selected year illustrated the usefulness of the approach. In fact, the interpretation of climatic wave statistics in terms of specific wave-regime scenarios facilitated a physical interpretation of the data. For example, the seasonal analysis for the representative year showed that all identified scenarios were present in all seasons but with different percentages of occurrence: S swells (scenario 5) were dominant in autumn and winter; however, scenarios that involve waves from the E quadrant (scenarios 1 and 2) dominate in summer and spring, with E swells (scenario 1) prevailing in spring and E seas (scenario 2) in summer.

We believe that interpreting wave climate statistics according to their wave-regime scenarios, besides providing a physical link between waves and winds, can open new possibilities for coastal studies and coastal engineering. For example, this approach could be used to improve the understanding of coastal processes by analyzing how the coast responds to each wave regime. It is also possible to investigate extreme conditions for each wave system separately and to relate them to their specific meteorological patterns.

LITERATURE CITED

Alves, J.H.G.M. and Melo, E., 1999. On the measurement of directional wave spectra at the southern Brazilian coast. *Applied Ocean Research,* 21(6), 295–309.

Alves, J.H.G.M. and Melo, E., 2001. Wind waves at the northern coast of Santa Catarina. *Revista Brasileira de Oceanografia,* 49(1/2), 13–28.

Araujo, C.E.S.; Franco, D.; Melo, E., and Pimenta, F.M., 2003. Wave regime characteristics of the southern Brazilian coast. *In: Proceedings of the Sixth Coastal and Port Engineering in Developing Countries* (COPEDEC VI Paper 097, Colombo, Sri Lanka), 15 pp.

Barletta, R.C., 1997. Morphodynamic Aspects of Beaches Located North of the Mouth of the Laguna dos Patos–Conceição Lighthouse and Adjacent Beaches: Final Paper, Curso de Oceanologia. Rio Grande do Sul, Brazil: Federal University of Rio Grande. [in Portuguese]. 54p.

Bijnen, E.J., 1973. *Cluster Analysis: Survey and Evaluation Techniques: Tilburg Studies on Sociology*, Volume 1. Tilburg, Netherlands: Institute for Labour Studies, Tilburg School of Economics, Social Sciences and Law. 124p.

Calliari, L.J.; Speranski N.S., and Boukareva, I.I., 1998. Stable focus of wave rays as a reason of local erosion at the southern Brazilian coast. *In:* Finkl, C.W. and Bruun, P. (eds.), *International Coastal Symposium (ICS) 1998 Proceedings*. Journal of Coastal Research, Special Issue No. 26, pp. 19–23.

Camus, P.; Méndez, F.J., and Medina, R., 2011. A hybrid efficient method to downscale wave climate to the coastal areas. *Coastal Engineering,* doi: 10.1016/j.coastaleng.2001.05.007.

Cuchiara, D.C.; Fernandes, E.H.; Strauch, J.C.; Winterwerp, J.C., and Calliari, L.J., 2009. Determination of the wave climate for the southern Brazilian shelf. *Continental Shelf Research,* 29(3), 545–555.

Machado, A.A.; Calliari, L.J.; Melo, E., and Klein, A.H.F., 2011. Historical assessment of extreme coastal sea state conditions in southern Brazil and their relation to erosion episodes. *Pan-American Journal of Aquatic Sciences,* 5(2), 277–286.

Melo, E.; Pimenta, F.M.; Mendes, D.A.R.; Hammes, G.R.; Araujo, C.E.S.; Franco, D.; Alves, J.H.G.M.; Barletta, R.C.; Souto, A.M.C.; Castelão, G.P.; Pereira, N.C., and Branco, F.V., 2003. A real time, on-line coastal information program in Brazil. *In:* Proceedings of the Sixth International Conference on Coastal and Port Engineering in Developing Countries, (COPEDEC VI, Paper 104, Colombo, Sri Lanka), pp. 14. [Published on compact disk].

Melo, E., 2004. Coastal information program: an overview of the first two years of operation. *In: The 1st Seminário e Workshop em Engenharia Oceânica*. Rio Grande do Sul, Brazil: SEMENGO, Federal University of Rio Grande, pp. 25. [in Portuguese]. http://www.semengo.furg.br/2004/39_2004.pdf

Melo, E.; Hammes, G.R.; Franco, D., and Romeu, M.A.R., 2008. Evaluation of the PERFORMANCE of the WW3 model in Santa Catarina. *In: The third Seminário e Workshop em Engenharia Oceânica*. Rio Grande do Sul, Brazil: SEMENGO, Federal University of Rio Grande, pp. 20. [in Portuguese]. http://www.semengo.furg.br/2008/08.pdf

Melo, E.; Romeu, M.A.R., and Hammes, G.R., 2010. Extreme sea state conditions off Rio Grande based on the WW3 model. *In: The Fourth Seminário e Workshop em Engenharia Oceânica*. Rio Grande do Sul, Brazil: SEMENGO, Federal University of Rio Grande, pp. 20. [in Portuguese]. http://www.semengo.furg.br/2010/23.pdf

Pianca, C.; Mazzini, P.L., and Siegle, E., 2010. Brazilian offshore wave climate based on NWW3 reanalysis. *Brazilian Journal of Oceanography,* 58(1), 53–70.

Strauch, J.C. and Schimidt, R.M., 1998. One year monitoring of waves in Rio Grande. *In: The XI Semana Nacional de Oceanografia: Oceanografia e suas interfaces, Resumos Expandidos*. Rio Grande do Sul, Brazil: Fundação Universidade Federal de Rio Grande. [in Portuguese], pp. 357–359.

Tolman, H.L., 2002. User Manual and System Documentation of Wave-Watch III. Version 2.22. College Park, MD: NOAA/NWS/NCEP/OB Technical Note 222, 133 pp.

Tomazelli, L.J., 1993. The wind regime and the rate of migration of coastal dunes wind of Rio Grande do Sul, Brazil. *Pesquisas,* 20(1), 18–26. [in Portuguese].